SINGLE POTASSIUM CHANNELS WITH DELAYED RECTIFIER BEHAVIOR FROM LOBSTER AXON MEMBRANES

ROBERTO CORONADO AND RAMON LATORRE
Department of Physiology and Biophysics, Harvard Medical School, Boston, Massachusetts 02115

HENRY G. MAUTNER
Department of Biochemistry and Pharmacology, Tufts University School of Medicine, Boston, Massachusetts 02114

ABSTRACT Single-channel potassium currents from lobster axon membranes were studied in planar bilayers made from monolayers. Channel-opening events are grouped by time, forming bursts with an average duration of 4.5 ms. The mean open time at 0 mV is 1.8 ms. The frequency of bursts is voltage dependent, increasing *e*-fold per 12–16 mV. At sufficiently high positive voltages, channels inactivate. Measured from reversal potentials, channels discriminate against Na^+ by a permeability ratio P_{Na}/P_K of 1:30. The channel is blocked by tetraethylammonium and nonyltrimethylammonium in a voltage-dependent manner and at concentrations similar to those used in whole-axon experiments. Voltage-dependent block by Cs^+ suggests that more than one ion may occupy the channel simultaneously. The kinetics and selectivity of this channel suggest that purified axolemma contains active K^+ channels that are likely to participate in delayed rectification in the lobster axon membrane.

INTRODUCTION

Reconstitution of single channels from purified membranes in planar phospholipid bilayers provides a way to learn about the functional state of channels removed from the intact cell. The planar bilayer offers a simple and defined environment in which the gating and conduction processes can be studied in detail (Latorre and Miller, 1983; Latorre et al., 1984; Miller, 1983).

The extent to which planar bilayers may contribute to the biochemical knowledge of nerve axon single channels is potentially large. Axolemmae devoid of gross contamination from Schwann membrane have been purified from retinal axons and crustacean leg nerve bundles (Zambrano et al., 1971; Balerna et al., 1975). Reconstitution of axon membrane fragments can be implemented in small bilayers formed in patch-clamp pipettes, increasing enormously the time and current resolution (Coronado and Latorre, 1983 *a*, *b*). In addition, there exists a detailed repertoire of axon Na^+- and K^+-channel properties that can be used to determine the integrity of axon channels in planar bilayers (Hodgkin and Huxley, 1952; Armstrong, 1975; Hille, 1975).

How "healthy" the axon Na^+ and K^+ channels in isolated axolemmae are is a question that must be answered in advance of further biochemical work. Na^+ channels may be active in lobster axolemmae, as indicated by flux assays (Condrescu and Villegas, 1982); however, no data exist for K^+ channels. We describe here the steady-state properties of single-channel K^+ currents from lobster walking-leg nerves detected in planar bilayers made from monolayers. The recorded single-channel currents include features such as bursting, voltage dependence, and voltage inactivation, that are in many ways similar to those described for single delayed-rectifier channels in squid axons using patch electrodes (Conti and Neher, 1980; Llano and Bezanilla, 1983). Further study of the selectivity and pharmacology of lobster channels in bilayers revealed an almost one-to-one correspondence with the selectivity and pharmacology of delayed rectifiers of nerve (Bezanilla and Armstrong, 1972; Hille, 1975; Adelman and French, 1978).

As judged from the bilayer results, purified lobster axolemma contains active K^+ channels for which most of the delayed rectifier properties may be preserved after insertion into planar bilayers. These findings make it particularly worthwhile to pursue, in the same system, the purification of the axon K^+ channel peptide(s). A study of K^+ channels in native membrane fragments is a first and necessary step.

MATERIALS AND METHODS

Bilayers were made by the monolayer assembly method (Montal and Mueller, 1972). Fig. 1 *A* shows a scheme of membrane assembly and recording conditions. Each chamber had a volume of 100 μl and the

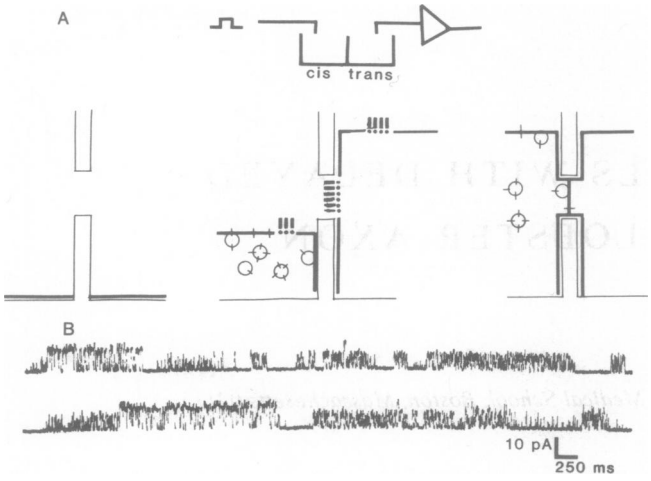

FIGURE 1 Assembly of bilayers from monolayers and recordings of channels at low time resolution. *A*, diagrams showing the three steps of bilayer assembly. *Left*, the chamber is coated with lipids and dried under N_2; *Middle*, the *trans* monolayer is lifted above the apperture with K^+ buffer; and afterwards *Right* the *cis* monolayer is lifted with K^+ buffer and vesicles. *B*, recordings correspond to contiguous traces at zero mV in 0.5 M KCl, 5 mM $CaCl_2$, 5 mM HEPES-Tris, pH 7.2 *cis*, and 0.1 M KCl, 5 mM HEPES-Tris, pH 7.2 *trans*.

aperture in the film (Teflon, 13-μm thick) is 80 μm in diam. Voltage pulses were injected in the front or *cis* chamber (see Fig. 1 *A*) via Ag/AgCl electrodes and current was collected and amplified in the back or *trans* chamber using a single-stage amplifier (LF-157AH, National Semiconductor, Santa Clara, CA). The reference voltage on the amplifier was maintained at ground voltage. The frequency response of the amplifier was 12 KHz. At 1 KHz, the current noise in bilayers of 120–150 pF was typically 1 pA peak-to-peak.

Axon membrane vesicles were incorporated by a vesicle-bilayer fusion procedure, enhanced by acid phospholipid, Ca^{2+} ions, and by an osmotic gradient (*cis* side made hyperosmotic) (Miller, 1978; Cohen et al., 1980) A protocol was developed to minimize exposure of vesicles to lipid solvents and to combine formation of bilayers and addition of axon vesicles into a single step. The bottom of each chamber was coated with a thin film of phospholipid, usually brain phosphatidylethanolamine (PE) and brain phosphatidylserine (PS) (Avanti Polar Lipids, Birmingham, AL) at a molar ratio of 1:1. In some experiments, a mixture of PE:phosphatidylcholine (PC):PS = 1:1:0.2 was used. The film of lipid was formed by thoroughly drying 1 mg of lipid under N_2 on each chamber. Monolayers at the air/water interface spontaneously formed after the chambers were filled with solutions. The *trans* monolayer was lifted above the aperture with a solution of 100 mM KCl, 10 mM HEPES-Tris, pH 7.5. The *cis* monolayer was lifted with a suspension of vesicles, usually 100 μg protein/ml in 0.5 M KCl, 0.5 mM $CaCl_2$, 10 mM HEPES-Tris, pH 7.5. The partition was pretreated with a solution of hexadecane (0.1%) in pentane.

Axon fragments were obtained from lobster walking-leg nerves by a modification of the procedures of Denburg (1972) and Balerna et al. (1975). Usually, 2 g of sensory motor nerve bundles were excised by the pulling method from the meropodite and carpopodite sections of 30–40 walking legs. All work was done at 4°C. Nerves were cut with scissors and homogenized in a ground-glass homogenizer with 10 vol of 0.32 M sucrose, 50 mM KCl, 10 mM Tris-Cl, pH 7.8. The homogenate was spun at 10,000 *g* for 15 min to remove debris and mitochondria. The pellet was rehomogenized in 1/3 the original volume and spun again at 10,000 *g*. The supernatants from the first and second spin were combined and made up to 20 mM in Mg^{2+} with a stock solution of $MgSO_4$. The suspension was spun at 100,000 *g* for 90 min to sediment the total fraction of microsomes. The total microsomal pellet was resuspended by homogenization in a glass-Teflon homogenizer in 20 ml of 5% sucrose (146 mM) buffered with 50 mM KCl, 10 mM Tris-Cl, pH 7.8. Membranes resuspended in 5% sucrose were spun at 10,000 *g* to remove aggregates. Supernatant (3.5 ml) was loaded on top of each of six discontinuous gradients containing a bottom layer of 40% sucrose (1.2 M) and a middle layer of 25% sucrose (0.73 M). All sucrose layers were buffered with 50 mM KCl, 10 mM Tris-Cl, pH 7.8. Gradients were spun for 16 h in an SW-40 rotor at 35,000 rpm. Axonal membranes sediment in the interface of 5%–25% sucrose. Membranes were diluted to 180 ml with 50 mM KCl, 10 mM Tris-Cl, pH 7.8 and spun at 100,000 *g* for 90 min. Pellets were resuspended in 0.5 M sucrose, 50 mM KCl, 10 mM Tris-Cl, pH 7.8 at a concentration of 5–10 mg protein/ml and stored at −80°C. 2 g of lobster nerves usually yielded 20 mg of purified membranes.

Data on axon K^+ channels comprise a total of 77 recordings using six different membrane preparations. Records were taken on FM tape (Racall-Lockheed, Sarasota, FL) at the full bandwidth of the current-to-voltage converter (12 KHz), and later played back and filtered using a low-pass four-pole filter (Krohn-Hite Corp., Avon, MA). Data were digitized in a TW-1117 signal processor (Tracor Northern, Madison, WI) and analyzed in a Hewlett-Packard microcomputer (Hewlett-Packard Co., Palo Alto, CA). The digitization rate was effectively increased by taping data at 60 in./s (20 KHz) and subsequently feeding records at low tape speed into the digitizer. Single-channel kinetics (Figs. 3 and 4 and Table I) were analyzed from records in which overlapping of events due to simultaneous opening of two or more channels did not occur. In the analysis, selected segments of 10-s recording time were digitized at 10 points/ms after records were filtered at both 4.5 KHz and 350 Hz (corner frequency). The low cut-off frequency was empirically found to eliminate the short closed flickers from the population of closed events. Elimination of short-lived closed events simplified the analysis of gating. Open and closed states were identified by setting a discriminator voltage at 50% below the mean open-state current. Changing the position of the discriminator ± 5% from this middle value did not distort open and closed distributions. Probability distribution histograms (Ehrenstein et al., 1974) were constructed separately from open and closed times by setting up a time array for measured dwell times. Mean times in Table I and Figs. 3 and 4 were obtained from best-fitted semilog curves using a least-squares regression. Data in Table II, and Figs. 5–7 were computed from chart records, usually filtered at 1 KHz. Entries correspond to mean open-channel conductance with SE within ± 5% from the mean. Two or more data points on a single *I-V* curve at the same voltage correspond to sets of data from different experiments. Reversal potentials in Table II are accurate within 5–10% depending on the experiment.

RESULTS

Single-Channel Kinetics

Fig 1 *B* shows the two kinds of unitary single-channel currents that can be detected in KCl media from our preparation of lobster vesicles. At zero mV, in a KCl gradient of 0.5 M *cis*/0.1 M *trans*, we often record large unitary jumps 12 pA in amplitude. We have not studied this channel in detail, but it probably corresponds to the channel that gives rise to a voltage-independent macroscopic K^+ conductance previously reported in Mueller-Rudin films from a similar preparation of vesicles (Coronado et al., 1981). The smaller unit currents 6–7 pA in amplitude, shown in Fig. 1 *B*, are the focus of our study. This channel is characterized by segments of fast transitions which, when compressed in time as in Fig 1 *B*, give rise to unresolved spikes. Spikes are alternated with long periods of inactivity. Fig. 2 *A* shows that each spike is a

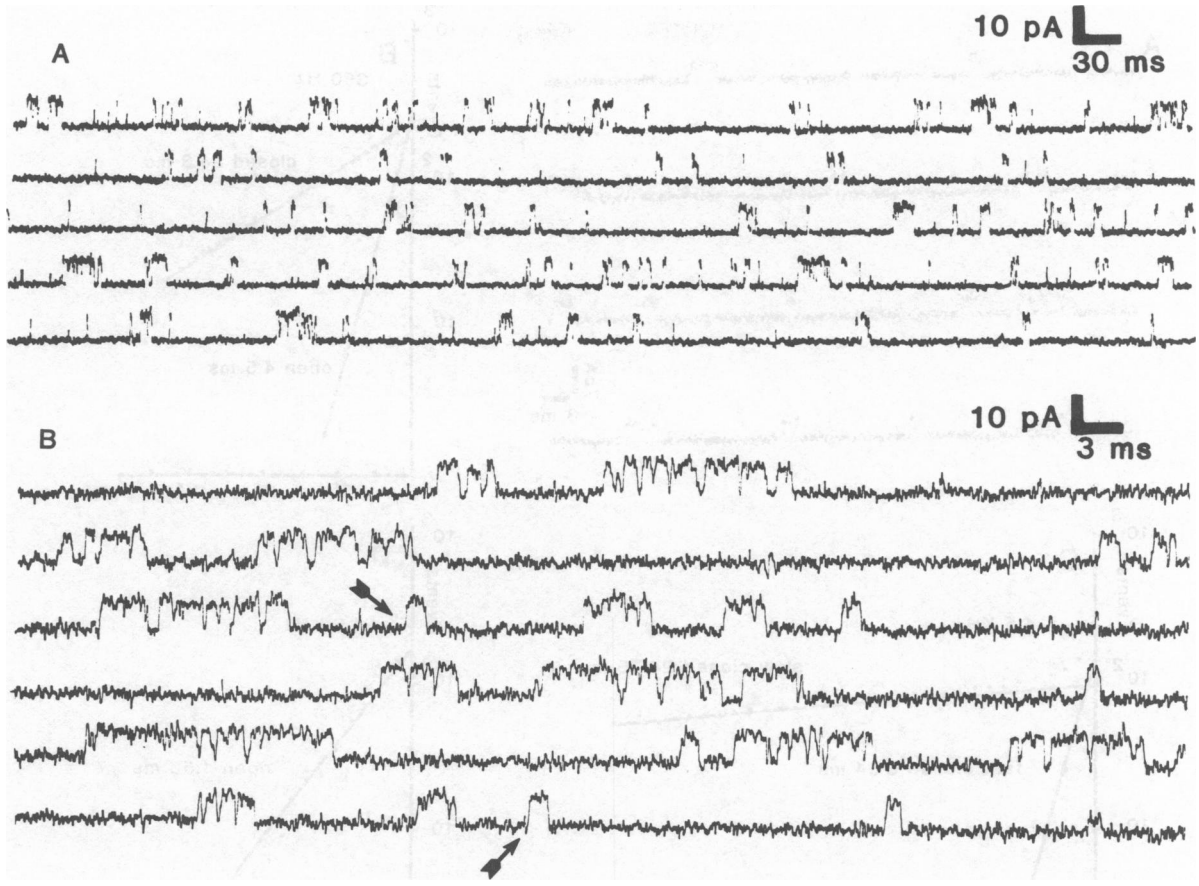

FIGURE 2 Bursting behavior of single channels. Traces in *A* and *B* are from the same bilayer at 4.5-KHz and 9-KHz filtering, respectively. Recordings are at a holding voltage of zero mV, 0.5 M CKl *cis* and 0.1 M KCl *trans*. Temperature of the experiment was 22°C. *A* is a continuous trace, while *B* corresponds to selected stretches from *A*.

brief and discrete square pulse of current lasting an average of 4–10 ms. Fig. 2 *B* shows that each spike is formed by a collection of consecutive openings interrupted by short closures. In what follows, we define such a collection of openings and closures separated by relatively long periods of inactivity as a "burst." It is apparent from the recordings of Fig. 2 *B*, however, that not all openings lead to bursts, inasmuch as some events (marked by arrows) consist of openings that are not followed by short closures but by long closed states.

The mean lifetime of openings and interruptions within bursts was measured from Poisson histograms of the cummulative distributions of dwell times (Ehrenstein et al., 1974). By measuring dwell times at low filtering frequencies, it is possible also effectively to filter out the fast closures within bursts and thus estimate the duration of bursts. Fig. 3 shows digitized data at 4.5 KHz and semilog histograms for open and closed times for the same set of data filtered at 4.5 KHz and 350 Hz. At 4.5 KHz, the distribution of closed times (Fig. 3 *C*) can be decomposed into a fast-closed lifetime of 0.5 ms and a slow-closed lifetime of 24.5 ms. At 350 Hz, the closed distribution (Fig. 3 *B*) does not contain fast-closed dwell times; the single component corresponds to the slow-closed component of 24.3 ms. This result indicates that the slow-closed component must originate without contamination from the interburst period, while the fast-closed component, eliminated at low cut-off frequencies, originates from the short interruptions within bursts. From the same records, the open distribution at 4.5 KHz shows a single component of 1.5 ms (Fig. 3 *D*), which is increased to 4.5 ms at 350 Hz (Fig. 3 *B*). This is expected because at low frequencies what is measured as open events is the uninterrupted lifetime of the whole burst, necessarily longer than the individual "true" lifetime of the open events. Data from several membranes at the same voltage are given in Table I. Some of the constructed histograms of open events show an additional fast-open component, $\leq$0.4 ms, that is too short to be evaluated here. The mean duration of the fast closures as well as of the mean open times is approximately the same for different experiments, with average values of 0.4 ms for the fast closures and 1.8 ms for the mean open time. Most of the variability within experiments is found in the density of mean frequency of recorded events, perhaps due to a variable number of channels in the bilayer. This is reflected in the duration of the interburst periods (slow

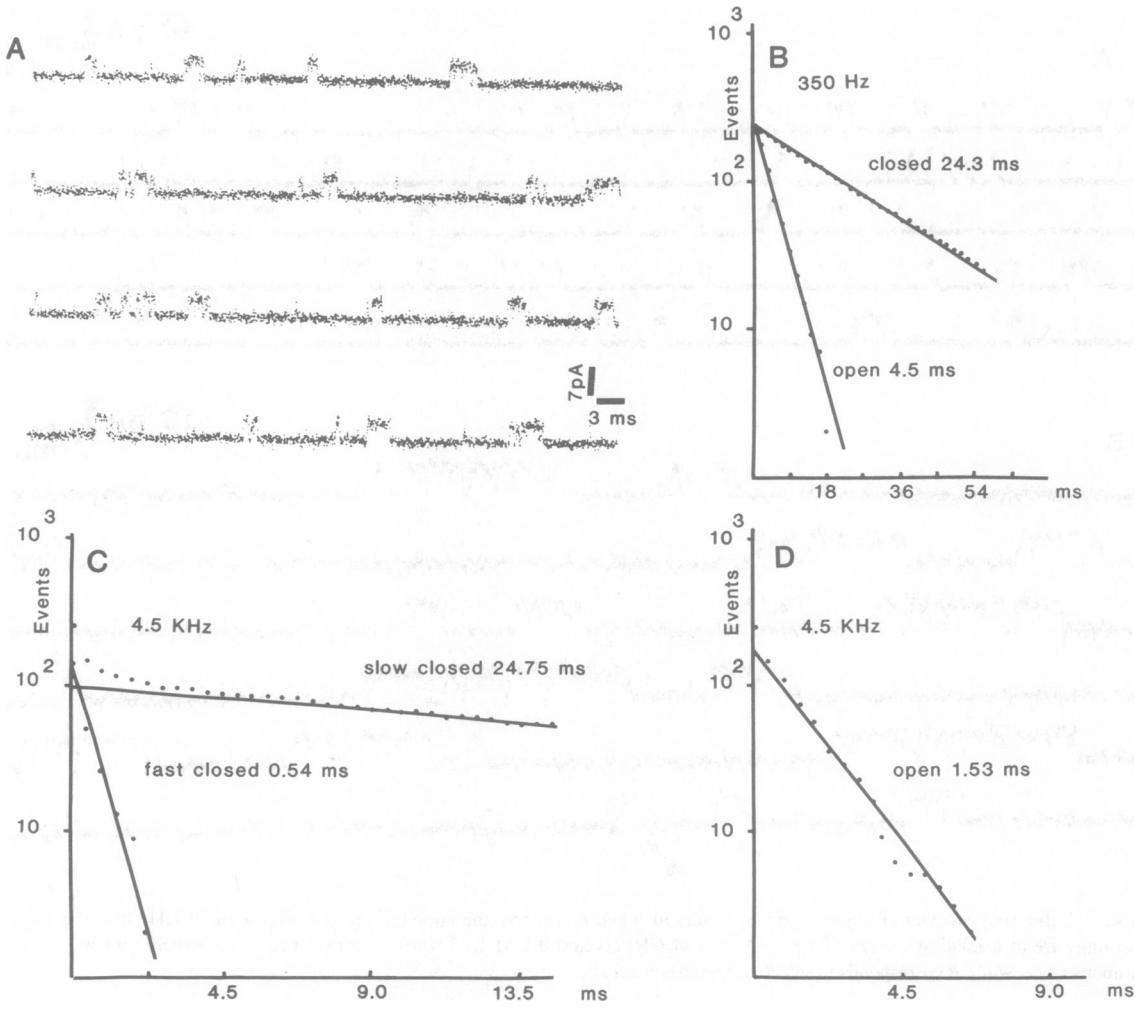

FIGURE 3 Histograms of closed and open dwell times. Recordings filtered at 4.5 KHz were digitized at 10 points/ms (*A*) to construct histograms of closed- and open-time distributions. In these curves, "events" correspond to the cummulative distribution of closed or open times longer than *t*, plotted in a semilog form vs. *t*. *B* shows open and closed distributions at 350 Hz; *C* and *D* are distributions of closed states and open states.

TABLE I
LIFETIME DISTRIBUTIONS OF LOBSTER POTASSIUM CHANNELS

Experiment	Events Measured	Open		Closed		Frequency of Events
		Fast	Slow	Fast	Slow	
		ms	*ms*	*ms*	*ms*	s^{-1}
Exp. 44						
0 mV; 4.5 KHz	455	0.36	2.61	0.405	4.23	278
Exp. 72						
0 mV; 4.5 KHz	255	not measurable	1.62	0.41	6.48	172
Exp. 34						
0 mV; 4.5 KHz	245	0.36	1.53	0.54	24.75	106
Exp. 34						
0 mV; 350 Hz	250	not measurable	4.5	not measurable	24.3	30

Data from several experiments at the same voltage (zero mV) and ionic conditions of Fig. 2. Entries are the mean times from histograms as in Fig. 3. Measured events correspond to the total counted number of openings included in the histograms.

closings), the longest interburst period for the experiments showing the lowest frequency of measurable events.

Channel Voltage Dependence

The effect of steady-state voltages on lobster K^+ channels was analyzed from single-channel records in bilayers in which the holding voltage was maintained constant for 10–15 s at each of the voltages considered. Fig. 4 *A* shows that positive potentials increase the total fraction of conducting time, g_{rel}, measured by dividing the open time in a given record by the total recorded time. The g_{rel} vs. voltage curve is the best single-channel equivalence to the macroscopic *n* curve (Hodgkin and Huxley, 1952). As such, it can be compared with voltage-clamp data from axon K^+ channels. The g_{rel} vs. *V* curve of lobster K^+ channels increases with voltage by *e*-fold per 12–16 mV, depending on the experiment, in the voltage range of −40 to +50 mV, a voltage sensitivity that is about fourfold lower than that of the squid K^+ channel (*e*-fold per 4 mV; Hodgkin and Huxley, 1952) but similar to that of the crab giant axon K^+-channel system (*e*-fold per 15 mV; Quinta-Ferreira et al., 1982). Unlike the macroscopic *n* curve, the curve for lobster K^+ channels is biphasic, showing a pronounced decline or inactivation of g_{rel} at high positive potentials. The increase in g_{rel} can be decomposed into an increase in the frequency of bursts (*e*-fold per 16 mV) and a much less sensitive (*e*-fold per 55 mV) increase in the duration of bursts (Fig. 4 *B*). Almost all of the voltage dependence resides in the mean frequency of bursts reproducing the shape of the g_{rel} curve in the whole range of voltages studied. The duration of bursts (also included in Fig. 4 *B*) is a monotonic function of voltage that does not contribute to the decrease in g_{rel} observed at large positive potentials.

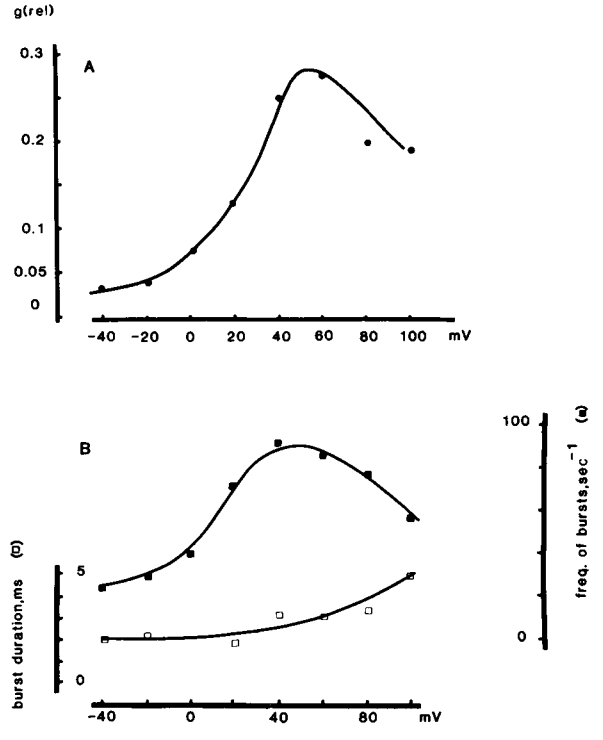

FIGURE 4 Steady-state voltage-dependence of lobster single channels. Data from a single membrane (1,800 individual openings at eight voltages) were used to reconstruct the voltage-dependence of the fraction of conducting time (*A*) and the frequency and duration of bursts (*B*). *A*, the fraction of conducting time measured by feeding 2-s records of single channels into a pulse-height analyzer and by computing the relative occurrence of the open and closed peaks. *B*, plot of the average frequency of bursts and mean duration of bursts. Burst duration was measured as in Fig. 3 *B*, by filtering records at 350 Hz.

Ionic Selectivity and Blockade

Lobster K^+ channels in bilayers completely exclude Cl^- ions, behaving like a perfect K^+ electrode. A plot of reversal potential vs. log of KCl *cis*/*trans* activity ratio has a slope of 61 mV (not shown). Fig. 5 shows single channel current-voltage curves under biionic conditions set up to measure the Na^+ permeability. In Fig. 5 *A*, the *cis*

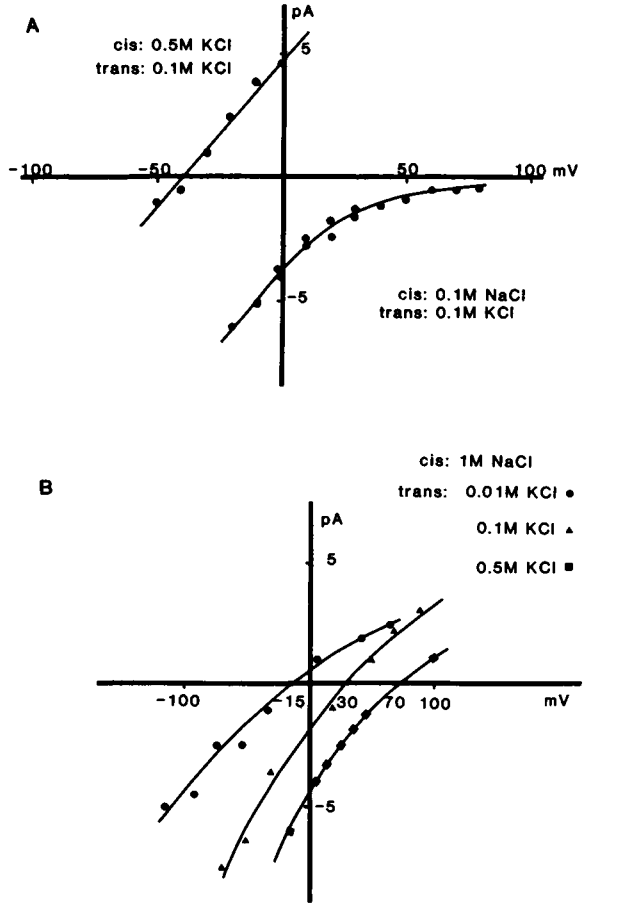

FIGURE 5 Current-voltage curves in the presence of *cis* sodium. *A*, current-voltage curves for channels in 0.5 M K^+ *cis*/0.1 M K^+ *trans* and after removal of *cis* K^+ and replacement with 0.1 M NaCl *cis*. Under these biionic conditions, the Na_+ reversal potential is >120 mV. *B*, sodium current through the channel measured after increasing *cis* Na^+ to 1 mM. The three curves for different *trans* K^+ are from different membranes. Reversal potentials in *B* are −15 mV in 10 mM K^+ *trans*. Solid lines are best-fitted curves.

solution was changed to 0.1 M NaCl after measuring a K^+ over Cl^- reversal potential of −40 mV in KCl 0.5 M *cis*/0.1 M *trans*. Under biionic Na^+/K^+ conditions, currents are negative, indicating a larger *trans*-to-*cis* K^+ current through the channel that becomes smaller at positive potentials. For the strict biionic Na^+/K^+ case, a reversal potential cannot be easily found since it lies at very large positive potentials. Sodium currents through the channel are measured in Fig. 5 *B* after increasing *cis* Na^+ and decreasing *trans* K^+ using three different ionic regimes. Reversal potentials and relative permeabilities calculated from the Goldman-Hodgkin-Katz equation are given in Table II for alkali cations NH_4^+ and Tl^+. Only Tl^+, K^+, Rb^+ and NH_4^+ are significantly permeant through the channel. Na^+ reversal potentials are all in agreement with an estimate of P_{Na}/P_K on the order of 1:30. Cs^+ ions, on the other hand, are the most impermeant, showing no sign of reversal potential even at a Cs^+/K^+ gradient of 10:1 (see also Fig. 6). The Cs^+ permeability is estimated at $<<0.01$, but it is likely that this ion may be impermeant in this channel by virtue of its blockade properties described below.

Blockade of delayed rectifiers by Cs^+ ions, tetraethylammonium (TEA) and derivatives such as nonyltrimethylammonium (C_9), has been characterized thoroughly (Armstrong, 1975; Adelman and French, 1978; Swenson, 1981; French and Shoukimas, 1981). These blockers also exert the same action on the lobster channel in bilayers. Cs^+ blockade is apparent here from the discontinuity in the current-voltage curve under biionic Cs^+/K^+, in the vicinity of the reversal potential (Fig. 6 *A*), and from single-channel conductance measured in mixed solutions of K^+ and Cs^+ (Fig. 6 *B*). In the former case, reversal at +60 mV

TABLE II
PERMEABILITY RATIOS FOR MONOVALENT CATIONS IN LOBSTER POTASSIUM CHANNEL CALCULATED FROM REVERSAL POTENTIALS OF SINGLE-CHANNEL CURRENTS

P_{ion}/P_K	Ion	*Cis* Solution	*Trans* Solution	V(rev)
				mV
3.3	Thallium	0.1 M TlAc	0.1 M KAc	−30
1.0	Potassium	—	—	—
0.63	Rubidium	1.0 M RbCl	0.1 M KCl	−40
0.1	Ammonium	0.5 M NH_4Cl	0.1 M KCl	+20
—	Sodium	0.1 M NaCl	0.1 M KCl	not measurable
0.027	Sodium	1.0 M NaCl	0.01 M KCl	−15
0.036	Sodium	1.0 M NaC	0.1 M KCl	+30
0.031	Sodium	1.0 M NaCl	0.5 M KCl	+70
0.017	Lithium	1.0 M LiCl	0.1 M KCl	+44
—	Cesium	0.1 M CsCl	0.1 M KCl	not measurable
<<0.01	Cesium	1.0 M CsCl	0.1 M KCl	not measurable

Permeability ratios were calculated from concentrations given above corrected for ionic activities. KCl-agar bridges were used in all experiments. In calculations, the Cl permeability was taken as zero. The thallium salt used was acetate.

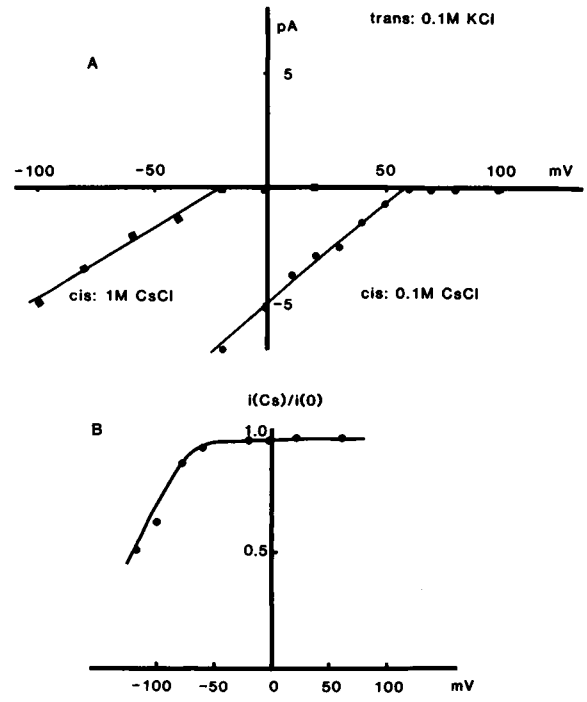

FIGURE 6 Lack of Cs^+ current and blockade of K^+ conductance of Cs^+. Single-channel current-voltage curves were measured in *A* under biionic conditions of 0.1 M K^+ *trans*/0.1 M Cs^+ *cis* and at 0.1 M K^+ *trans*/1.0 M Cs^+ *cis*. In *B*, the blockade of potassium currents was measured in the presence of symmetrical solutions of 0.1 M KCl + 50 mM CsCl. $i(Cs)/i(o)$ is the ratio of single-channel currents in the presence of K^+, Cs^+ and $i(o)$ is the unblocked conductance measured at +60 mV. The solid line (—) was drawn according to Eq. 1 with Kd = 200 mM and $z\delta$ = 1.3.

can be obtained by extrapolation, but measurements up to +100 mV show no Cs^+ current. If any Cs^+ current exists, it must be lower than the noise limit in the bilayer (1 pA at 1 KHz). In the latter case, blockade is expressed in the amplitude of single-channel currents measured under constant ionic strength and symmetrical solutions in the presence of Cs^+. At negative potentials, the conductance of single channels decreases in a voltage-dependent manner, indicating a predominant *trans* block by Cs^+. No *cis* block by Cs^+, under the conditions of Fig. 6 *B*, are observed up to +60 mV. A convenient measure of blockade is obtained by fitting data according to the equation (Woodhull, 1973):

$$i/i_o = \left[1 + \frac{[Cs^+]}{K_d} \exp \frac{(z\delta FV)}{RT}\right]^{-1} \quad (1)$$

where i/i_o is the ratio of blocked/unblocked channel current, K_d is an apparent dissociation constant of Cs^+ from the channel, $z\delta$ is the effective valence of block, and R, T and F are the thermodynamic constants. The solid line of Fig. 6 *B* was drawn with K_d = 200 mM and $z\delta$ = 1.3. A $z\delta > 1$ is characteristic of delayed and inward rectifiers and has been taken to indicate occupancy of the channel by several ions (Hille and Schwartz, 1978). In this case, either two Cs^+ ions or a Cs^+ and a K^+ ion must coexist within the

electric field inside the channel to account for a valence larger than unity. High $z\delta$ with low affinity of block was also measured in the external Cs^+ block of squid delayed rectifiers (Adelman and French, 1978). Fig. 7 shows block by TEA and C_9 at the same range of concentrations used in squid experiments (Armstrong, 1975). Concentrations of 10 mM TEA and 100 μM C_9 decrease channel currents at positive voltages, i.e., a predominant *cis* block. The $z\delta$ of block for these compounds is 0.6, a value larger than that measured in the squid K^+ channel ($z\delta$ ~0.2, French and Shoukimas, 1981).

Single-Channel Conductance

Table III shows the single-channel conductance at different ionic conditions, with different lipids and at different potentials. Under symmetrical 0.5 M K^+ (Experiment 43), channels display linear current-voltage curves within ± 60 mV. Decrease in *trans* K^+ (Experiments 52, 25) or increase in *cis* K^+ (Experiment 56) produced voltage-dependent rectification of single-channel currents. The channel conductance increases in the direction of K^+ movement from the high to low concentration. Analysis of current-voltage curves for the steepest K^+ gradient (0.5 M *cis*/0.01 M *trans*) showed that rectification was not in excess of that predicted by the Goldman electrodiffusion equation (see Armstrong, 1975).

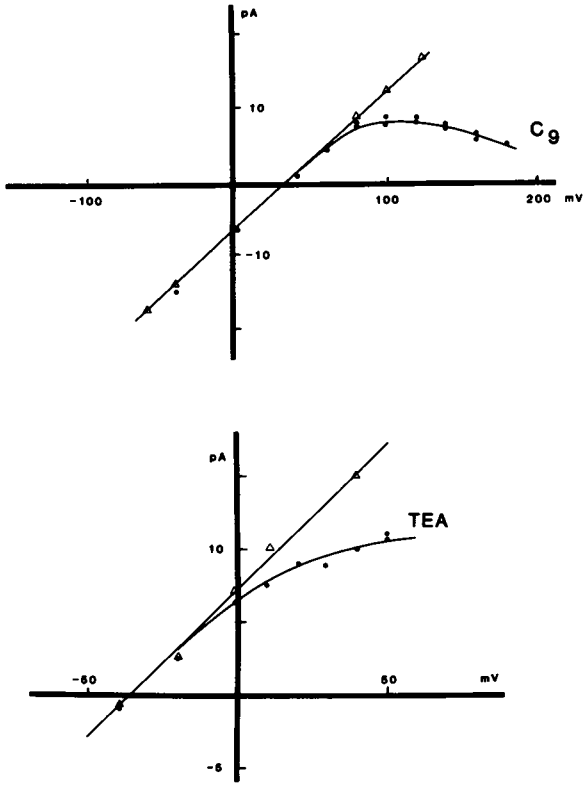

FIGURE 7 Block of single-channel K^+ currents by tetraethylammonium (TEA) and nonyltrimethylammonium (C_9). *A*, block by C_9 in 0.1 M K^+, 100 μM C_9 *cis*/0.5 M K^+ *trans*. The mean channel conductance in the range of −50 mV to +150 mV was measured after filtering single-channel events at 200 Hz (•). In the same membrane, control *I-V* curves were taken before addition of C_9 (△). *B*, block by TEA was measured in 0.1 M K^+ *cis*, 10 mM TEA/0.1 M K^+ *trans* (•). Control currents were measured using the same gradient, in the absence of TEA (△).

In bilayers using the phospholipids prevailing in the axon membrane (PC:PE:PS) at a molar ratio of 1:1:0.2 (Zambrano et al., 1971), and a K^+ gradient of 0.5 M K^+ *cis*/0.01 M *trans*, the channel has a conductance of 55 pS at 0 mV. Conti and Neher (1980) obtained a value of 17.5 ps for the delayed rectifier of squid axon at 5°C with the K^+ gradient reversed (i.e., 0.46 M K^+ outside, 0.001 M K^+ inside). From this value, they calculated that under physiological conditions the delayed rectifier should have a conductance of ~10 pS, which is close to that obtained from noise analysis (Conti et al., 1975). At 5°C and assuming a Q_{10} of 1.3 for the lobster K^+ channel, we obtain a conductance of 28 pS. This conductance is 2.8-fold larger than that of the K^+ channel in squid. However, in situ, it is possible that the lobster axon delayed-rectifier conductance can be lower than 28 pS. In this regard, at least two factors may influence the channel conductance. First, we notice that the lobster single-channel conductances are larger at high molar ratios of PS. Inasmuch as the axon membrane contains a molar ratio of phospholipid:cholesterol = 1:0.7, one would expect a decrease in the surface density of negatively charged PS in the axon membrane ~40% lower than that of the last experiments in Table III. If the trend of Table III continues, we expect that addition of cholesterol should decrease the channel conductance to a value below that found in bilayers formed from mixtures containing only phospholipids. Second, cholesterol per se may have an effect on the channel conductance. Both possibilities are now under study.

The general characteristics of channel gating are not modified by lipid composition. Therefore, a high molar ratio of PS was used in the present experiments to optimize the signal-to-noise ratio.

DISCUSSION

Channel-Gating Kinetics

Single-channel data on delayed rectifers are very limited. Patch clamp in axons is inherently difficult, owing to the high density of channels in the axon membrane. Nevertheless, Conti and Neher (1980) and recently Llano and Bezanilla (1983), recorded single potassium channels in squid. Their studies revealed new properties of channels otherwise masked by whole axon currents: the conducting potassium channel is formed by bursts of opening events separated by relatively long interburst periods. Table IV compares the lifetime of states intervening in the formation of bursts obtained by patch-clamp in squid with those obtained here in bilayers. Measured at depolarized voltages, the burst structure is the same for both channels. Short closures are much shorter than opening events and each burst contains, on the average, three closures. Several

TABLE III
EFFECT OF K^+ CONCENTRATION AND BILAYER PHOSPHOLIPID COMPOSITION ON LOBSTER POTASSIUM CHANNEL CONDUCTANCE

Experiment	Bilayer Phospholipid Composition*	Single Channel Conductance At Indicated Voltage‡			Reversal Potential§
		pS, mV			*mV*
Exp. 52					
0.5 M K^+ *cis*	PE:PS = 1:1	40, −120	55, −90	150, +60	−90
0.01 M K^+ *trans*					
Exp. 25					
0.5 M K^+ *cis*	PE:PS = 1:1	100, −80	153, −35	250, +60	−35
0.1 M K^+ *trans*					
Exp. 43					
0.5 M K^+ *cis*	PE:PS = 1:1	110, −60	110, 0	110, +60	0
0.5 M K^+ *trans*					
Exp. 56					
1.0 M Na^+ *cis*	PE:PS = 1:1	100, −20	70, +70	30, +100	+70
0.5 M K *trans*					
Exp. 68					
0.5 M K^+ *cis*	PS	140, −120	200, −95	280, 0	−95
0.01 M K^+ *trans*					
Exp. 66					
0.5 M K^+ *cis*	PE:PC:PS =	—	40, −90	55, 0	−90
0.01 M K^+ *trans*	1:1:0.2				

*Molar ratio of phospholipid mixture used to form bilayers; mixed fatty acid chain lipid from bovine brain.
‡Conductance at room temperature (22°–25°C) calculated from slope conductance at given voltage. Data from single-channel current-voltage curves fitted at 1 KHz.
§Single-channel reversal potentials measured from same experiment at the ionic gradients indicated. All solutions buffered with 10 mM Hepes-Tris, pH 7.5. Chloride salts were used in all experiments.

differences that must be mentioned make the comparison appropriate only in qualitative terms. Temperature, for example, might be responsible for the decrease in lifetimes in the lobster channel by a factor of three in all parameters except the number of flickers. However, more subtle effects arising from bilayer lipid and K^+ concentration (which we have not studied systematically) must also be considered.

From the analysis of records whose bursts are sufficiently separated in time, a minimum of two closed states and one (or two) open state(s) are essential to the kinetic mode of single channels (Table I). Additional states will be needed to account for the long closed intervals in the 100-ms time scale (see Fig. 1 *B*) and also for the termination or inactivation of bursts at high positive potentials. At this point, we can only guess, from steady-state data, how these states are connected and how the voltage dependence may arise. Several possibilities are clear from the following scheme, which is generally applicable to bursting channels,

$$C \cdots C \cdots C_2 \underset{k_{-2}}{\overset{k_2(V)}{\rightleftharpoons}} C_1 \underset{k_{-1}}{\overset{k_1}{\rightleftharpoons}} O \cdots C' \qquad (2)$$

$$\vdots \qquad \vdots \qquad \vdots$$

$$I$$

where *C* denotes closed, *O* open, and *I* inactive. Bursts in channels are indicative of two equilibrium processes connected by some common state and occurring in different time scales. Lobster K^+ channels burst either because *O* is in fast equilibrium with *C'* to the right and occasionally closes to C_1 (case C–O–C), or because *O* is in fast equilibrium with C_1 and occasionally closes to C_2 to the left (case C–C–O). In the absence of controlling variables,

TABLE IV
COMPARISON OF BURST STRUCTURE OF SQUID AND LOBSTER POTASSIUM SINGLE CHANNELS

	Burst Duration	Closures per Burst	Brief Openings	Brief Closures
	ms		*ms*	*ms*
Lobster channel in bilayers* 0 mV, 22°C	4.5	3.5	1.8	0.4
Squid channel, patch-clamp recordings‡ −25 mV, 5°C	12	3.0	3.5	1.3

*Averages of data from Table I; mean number of closures per burst was measured directly from records. The same number can be estimated from the ratio of the frequency of total closed events at 4.5 KHz (including flickers) and 350 Hz (excluding flickers).
‡Data from Conti and Neher, 1980.

such as an agonist, and when only steady-state data are considered, the two cases are indistinguishable (Colquhoun and Hawkes, 1981). A C–C–O model for the last steps leading to channel opening describes the macroscopic kinetics of K^+ channels in axons (Armstrong, 1971). In the absence of contradictory evidence, we favor the same scheme to explain flickering and voltage dependence. Voltage dependence in the lobster channel is manifested as an increase in the frequency of bursts at positive potentials without a major increase in the duration of bursts. Within a more limited range of voltages, the same description was made for squid channels (Conti and Neher, 1980). If burst duration is insensitive to voltage, the k_1/k_{-1} equilibrium must be largely independent of voltage. Most of the voltage dependence must reside, then, in some inner step leading to the formation of bursts: for example, in $k_2(V)$ controlling the $C_2 \rightarrow C_1$ transition. Actually, a C–C–O scheme demands that $k_2(V)$ be the rate-determining step if bursts are to be generated (Colquhoun and Hawkes, 1981). More recently, Bezanilla and White (1983) have been able to generate the time course of the macroscopic K^+ current and gating currents with a six-state linear model having five closed and one open state. In this model, the first step in the sequence is rate-limiting and the last (... closed → open) is the fastest step. The model also predicts the bursting channel behavior found here and by Conti and Neher (1980).

A complication in the analysis of lobster channels arises from the fact that steady positive voltages open channels but, at sufficiently large values, the channels close. An interpretation is that channels, for the long pulses (10 s) used to collect data, inactivate like K^+ channels in squid (Ehrenstein and Gilbert, 1966). We believe that this process is slow, since a decrease in the frequency of bursts is not obvious from our records. We do not know in our case if channels recover from inactivation by holding channels at negative voltages. It is noteworthy that, in the same voltage range where the frequency of bursts decreases steeplky, the duration of bursts continues to increase, as if inactivation were unable to proceed once a burst has been initiated. Thus, in the records used in Fig. 4, at voltages beyong +6-mV, there are fewer bursts per unit time but those bursts observed are of increasingly longer duration. Slow inactivation, as indicated in scheme 1, may proceed from any state (open or closed), but we prefer to think that (I) is reached from the slow closed states (C) based on the observation pointed out above.

Selectivity and Block

In addition to the kinetics, the selectivity of the lobster channel is remarkably similar to that of nerve K^+ channels. Axon K^+ channels show a pattern of permeability to alkali ions that is different from that of other cellular K^+ and, in particular, is different from the resting conductance. Table V compares the permeability ratios obtained in bilayers with the selectivity of squid and Node of Ranvier delayed rectifiers and squid resting conductance. In several excitable cells (see Hagiwara et al., 1972), the resting K^+ conductance is leaky to Cs^+ ions. This is quite in contrast to the bilayer lobster channel and delayed rectifiers of nerve where the lack of Cs^+ permeability results in a block of the channel. In the bilayer case, as in delayed rectifiers, there are only four ions that show high permeability: $Tl^+ > K^+ > Rb^+ > NH_4^+$. Also, the same low field-strength sequence of permeation holds for the three cases (Krasne and Eisenman, 1973). Other common features are found in the blockade by Cs^+, TEA, and C_9. Internal and external Cs^+, for example, block squid channels with a high valence of block: under some conditions, the valence is larger than unity (Adelman and French, 1978). A value of 1.3 was measured here for *trans* block by Cs^+. To a lesser extent, *cis* Cs^+ also blocks the "cytoplasmic" *cis*-end of the channel (not shown). A $z\delta > 1$ indicates that the channel contains more than one ion binding site that can be occupied simultaneously (e.g., Hille and Schwartz, 1978). TEA and C_9, in contrast to Cs^+, are predominantly *cis* blockers. As defined by the voltage dependence of the channel, the *cis* side is equivalent to the inner cytoplasmic entity. Thus, the sidedness of block for these compounds is the same as in nerve (Armstrong, 1975; but see Armstrong and Hille, 1972).

TABLE V
PERMEABILITY RATIOS P_x/P_{K^+} OF NERVE K^+ CONDUCTANCE

Ion	Resting* Conductance (Squid)	Delayed Rectifiers‡§‖¶ Squid	Delayed Rectifiers‡§‖¶ Node of Ranvier	Lobster Channel** in Bilayers
Tl^+	1.82	—	2.1	3.3
K^+	1.0	1.0	1.0	1.0
Rb^+	0.71	1.0	0.9	0.63
NH_4^+	0.2–0.3	0.2	0.13	0.1
Na^+	<0.08	0.03	0.01	0.03
Li^+	<0.08	<0.01	<0.02	0.017
Cs^+	0.18	<0.01	<0.08	<<0.01

Data from (*) Hagiwara et al., 1972; (§) Binstock and Lecar, 1969; (§) Baker et al., 1962; (‖) Bezanilla and Armstrong, 1972; (¶) Hille, 1975; (**) from Table II, present data.

We are grateful to Dr. M. T. Tosteson for the use of her computer. The expert secretarial help of Marianita Sanchez is warmly acknowledged.

This work was supported by National Institutes of Health grants GM-28992 to R. Latorre and GM-25277 to D. C. Tosteson, and by a postdoctoral fellowship to R. Coronado from the Muscular Dystrophy Association of America.

Received 28 April 1983 and in final form 16 June 1983

REFERENCES

Adelman, W. J., Jr., and R. J. French. 1978. Blocking of the squid axon potassium channel by external cesium ions. *J. Physiol. (Lond.)* 276:13–25.

Armstrong, C. M. 1971. Interaction of tetraethylammoium ion derivatives with the potassium channels of giant axons. *J. Gen. Physiol.* 58:413–437.

Armstrong, C. M. 1975. K^+ pores of nerve and muscle. *In* Membranes, A Series of Advances. G. Eisenman, editor. Marcel Dekker, Inc., New York. 3:325–358.

Armstrong, C. M., and B. Hille. 1972. The inner quaternary ammonium ion receptor in potassium channels of the node of Ranvier. *J. Gen. Physiol.* 59:388–400.

Balerna, M., M. F. Fosset, R. Chicheportiche, G. Romey, and M. Lazdunski. 1975. Contribution and properties of axonal membranes of crustacean nerves. *Biochemistry.* 14:5500–5511.

Bezanilla, F., and C. M. Armstrong. 1972. Negative conductance caused by the entry of sodium and cesium into potassium channels of squid axons. *J. Gen. Physiol.* 60:588–608.

Bezanilla, F., and M. White. 1983. Properties of ionic channels in excitable membranes. *In* Physiology of Membrane Disorders. T. E. Andreoli et al., editors. Plenum Publishing Corp., New York. In press.

Binstock, L., and H. Lecar. 1969. Ammonium ion currents in the squid giant axon. *J. Gen. Physiol.* 53:342–361.

Cohen, F. S., J. Zimmerberg, and A. Finkelstein. 1980. Fusion of phospholipid vesicles with planar phospholipid bilayer membranes. II. Incorporation of a vesicular membrane marker into the planar membrane. *J. Gen. Physiol.* 77:251–270.

Colquhoun, D., and A. G. Hawkes. 1981. On the stochastic properties of single ion channels. *Proc. R. Soc. Lond. B. Biol. Sci.* 211:205–235.

Condrescu, M., and R. Villegas. 1982. Ion selectivity of the nerve membrane sodium channel incorporated into liposomes. *Biochim. Biophys. Acta.* 688:660–666.

Conti, F., and E. Neher. 1980. Single channel recordings of K^+ currents in squid axons. *Nature (Lond.).* 285:140–143.

Conti, F., L. J. DeFelice, and E. J. Wanke. 1975. Potassium and sodium ion current noise in the membrane of the squid giant axon. *J. Physiol. (Lond.).* 248:45–82.

Coronado, R., and R. Latorre. 1983 *a*. Formation of lipid bilayer membranes on patch-clamp pipettes: a reconstitution technique for ionic channels. *Biophys. J.* 40(2,pt.2):56*a*. (Abstr.)

Coronado, R., and R. Latorre. 1983 *b*. Formation of phospholipid bilayers from monolayers in patch-clamp pipettes. *Biophys. J.* In press.

Coronado, R., R. Huganir, and G. Mautner. 1981. A K^+-selective conductance sensitive to cholinergic antagonists obtained by fusion of axonal membrane vesicles to planar bilayers. *FEBS (Fed. Eur. Biochem. Soc.). Lett.* 131:355–358.

Denburg, J. E. 1972. An axon membrane preparation from the walking legs of the lobster. *Biochim. Biophys. Acta.* 282:453–458.

Ehrenstein, G., and D. L. Gilbert. 1966. Slow changes of potassium permeability in the squid giant axon. *Biophys. J.* 6:553–565.

Ehrenstein, G., R. Blumenthal, R. Latorre, and R. Lecar. 1974. Kinetics of the opening and closing of individual excitability-inducing–material channels in a lipid bilayer. *J. Gen. Physiol.* 63:707–721.

French, R. J., and J. J. Shoukimas. 1981. Blockade of squid axon potassium conductance by internal tetra-*N*-alkylammonium ions of various sizes. *Biophys. J.* 34:271–292.

Hagiwara, S., Eaton, D. C., Stuart, A. E., and Rosenthal, N. P. 1972. Cation selectivity of Na and K channels of nerve membrane. *In* Membrane, A Series of Advances. G. Eisenman, editor. Marcel Dekker, Inc., New York. 3:256–323.

Hille, B., and W. Schwartz. 1978. Potassium channels as multi-ion single-file pores. *J. Gen. Physiol.* 72:409–442.

Hodgkin, A. L., and A. F. Huxley. 1952. A quantitative description of membrane current and its application to conduction and excitation in nerve. *J. Physiol. (Lond.).* 117:500–544.

Krasne, S., and G. Eisenman. 1973. The molecular basis of ion selectivity. *In* Membranes, A Series of Advances. G. Eisenman, editor. Marcel Dekker, Inc., New York. 3:277–328.

Latorre, R., R. Coronado, and C. Vergara. 1984. K^+ channels gated by voltage and ions. *Annu. Rev. Physiol.* In press.

Latorre, R., and C. Miller. 1983. Conduction and selectivity in K^+ channels. *J. Membr. Biol.* 71:11–30.

Llano, I., and F. Bezanilla. 1983. Bursting activity of potassium channels in the cut-open axon. *Biophys. J.* 41(2,pt.2):38*a*. (Abstr.)

Miller, C. 1978. Voltage-gated cation conductance channel from fragmented sarcoplasmic reticulum: steady-state electrical properties. *J. Membr. Biol.* 40:1–23.

Miller, C. 1983. Integral membrane channels: studies in model membranes. *Physiol. Rev.* In press.

Montal, M., and P. Mueller. 1972. Formation of bimolecular membranes from lipid monolayers and a study of their electrical properties. *Proc. Natl. Acad. Sci. USA.* 69:3561–3566.

Quinta-Ferreira, E., E. Rojas, and N. Arispe. 1982. Potassium currents in the giant axon of the crab *Carcinus maenas*. *J. Membr. Biol.* 66:171–181.

Swenson, R. 1981. Inactivation of potassium currents in squid axon by a variety of quaternary ammonium ions. *J. Gen. Physiol.* 77:255–271.

Woodhull, A. M. 1973. Ionic blockade of sodium channels in nerve. *J. Gen. Physiol.* 61:687–708.

Zambrano, F., M. Cellino, and M. Canessa-Fischer. 1971. The molecular organization of nerve membranes. IV. The lipid composition of plasma membranes from squid retinal axons. *J. Membr. Biol.* 6:289–303.

DISCUSSION

Session Chairman: Alan Finkelstein *Scribes*: John W. Hanrahan and Robert L. Rosenberg

MONTAL: It would be interesting first to test high-affinity reagents, such as the scorpion toxin purified by A. Maelicke, to identify the nature of the K^+ channel and to isolate pure channel protein.

CORONADO: There are few high affinity reagents for K^+ channels like those that helped in isolating ACh receptor and Na channels. Scorpion toxin would be a good one to try. This bilayer provides a good assay for testing high-affinity ligands which might be used in such purifications.

DEFELICE: You argue that the conductance of these channels is similar to that observed in squid axon if you take into account the effect of surface charge. Why should they be the same?

CORONADO: There are no noise data bearing on this in lobster nerve channels. Yes, channels from different sources may not be the same.

LABARCA: Do you have any problems with orientation?

CORONADO: Polarity is defined by the voltage-dependence. It is always the same.

LABARCA: Have you used detergents followed by detergent removal (i.e., dialysis)?

CORONADO: No.

ZIMMERBERG: Do you see any evidence with this preparation for inactivation, such as is seen in squid axon during very long pulses?

CORONADO: Yes. We see slow burst inactivation.

HARTSHORNE: Is there an effect of cholesterol on single-channel conductance?

CORONADO: I haven't examined this in detail yet.

FINKELSTEIN: What is your kinetic scheme and where is the voltage-dependent step?

CORONADO: There are three states: $C_2 \rightleftharpoons C_1 \rightleftharpoons O$. Transitions between O and C_1 produce the flickering, whereas excursions to C_2 result in interburst periods. The voltage-dependent step is between C_2 and C_1.

FINKELSTEIN: Is the voltage-dependent step from C_2 to C_1 or from C_1 to C_2?

LATORRE: Only the interburst period is affected. Because there is no change in the mean duration of brief closures, it must be the C_2-to-C_1 rate that is affected.

EHRENSTEIN: Do have any explanation for the decrease in current in the I-V curve at very depolarized potentials, seen in your single-channel results as well as in voltage-clamp experiments?

CORONADO: No.

YEH: Does bursting behavior increase in the presence of Ca^{++} or TEA? Does 4-AP have any effect?

CORONADO: There is more flickering with C_9 (it supplies flickers). At very high voltages, bursts get longer but we can't resolve fast flickers and the burst amplitudes appear to decrease. We haven't tried 4-AP.